Biochemical and Biophysical Research Communications 456 (2015) 269–274

Contents lists available at ScienceDirect

Biochemical and Biophysical Research Communications

journal homepage: www.elsevier.com/locate/ybbrc

Proteasome inhibitors induce auditory hair cell death through peroxisome dysfunction

Joon No Lee, Seul-Gi Kim, Jae-Young Lim, Se-Jin Kim, Seong-Kyu Choe, Raekil Park *

Center for Metabolic Function Regulation, Department of Microbiology, Wonkwang University School of Medicine, Iksan, South Korea

ARTICLE INFO

Article history:
Received 13 November 2014
Available online 25 November 2014

Keywords:
Proteasome inhibitor
Auditory hair cell
Peroxisome dysfunction
Hearing loss

ABSTRACT

Even though bortezomib, a proteasome inhibitor, is a powerful chemotherapeutic agent used to treat multiple myeloma (MM) and other lymphoma cells, recent clinical reports suggest that the proteasome inhibitor therapy may be associated with severe bilateral hearing loss. We herein investigated the adverse effect of proteasome inhibitor on auditory hair cells. Treatment of a proteasome inhibitor destroys stereocilia bundles of hair cells resulting in the disarray of stereocilia in the organ of Corti explants. Since proteasome activity may be potentially important for biogenesis and function of the peroxisome, we tested whether proteasome activity is necessary for maintaining functional peroxisomes. Our results showed that treatment of a proteasome inhibitor significantly decreases both the number of peroxisomes and expression of peroxisomal proteins such as PMP70 and Catalase. In addition, we also found that proteasome inhibitor impairs the import pathway of PTS1-peroxisome matrix proteins. Taken together, our findings support recent clinical reports of hearing loss associated with proteasome inhibition. Mechanistically, peroxisome dysfunction may contribute to hair cell damage and hearing loss in response to the treatment of a proteasome inhibitor.

1. Introduction

Peroxisomes contain more than 100 enzymes and other proteins to conduct cellular metabolic functions including very long and branched chain fatty acid oxidation, synthesis of bile acids and plasmalogen, conversion of hydrogen peroxide to nontoxic forms [1,2]. Mutations in genes involved in peroxisome biogenesis or peroxisomal function cause inheritable genetic disorders, such as Zellweger syndrome, infantile Refsum disease, neonatal adrenoleukodystrophy [3–5]. Peroxisomes are derived from the ER and undergo maturation by importing peroxisome matrix proteins from the cytosol through the specific peroxisome target sequence (PTS) [6]. For importing the matrix proteins into the peroxisome, several Pex proteins are participated in the process of peroxisome assembly. Among them, Pex2, 10, 12 are E3 ubiquitin ligase, and Pex5 acting as PTS receptor is subject to poly-ubiquitination and degradation by proteasome during peroxisome formation [7]. These findings suggested that proteasome function might be important for biogenesis and function of the peroxisome.

The ubiquitin-proteasome pathway plays an important role for intracellular protein degradation to regulate various cellular processes. The ubiquitin conjugating system is composed of ubiquitin activating enzymes (E1), ubiquitin conjugating enzymes (E2), ubiquitin ligases (E3), de-ubiquitinases and the 26S proteasome-containing multi-protease complex [8,9]. Inhibition of the proteasome function affects the active forms of proteins that regulate cell cycle progression, transcription, inflammation, apoptosis, and angiogenesis [10,11]. Bortezomib acting as proteasome inhibitor is an anticancer agent used to treat multiple myelolma (MM) [12]. However, recent reports showed that bortezomib therapy is associated with hearing loss [13,14]. Notably, a sensory deafness has been known as one of the clinical symptoms associated with peroxisome defects, such as Zellweger syndrome, infantile Refsum disease, acyl-CoA Oxidase deficiency, and D-bifunctional protein deficiency [15–18]. Therefore, we investigated a potential link between proteasome inhibition and peroxisome dysfunction which may result in hair cell damage and hearing loss.

2. Materials and methods

2.1. Cell culture and viability

Establishment and characterization of conditionally immortalized auditory HEI-OC1 cells have well been described. Cells were

* Corresponding author at: Department of Microbiology, Wonkwang University School of Medicine, 460 Iksan-daero, Iksan, Jeonbuk 570-749, South Korea. Fax: +82 63 855 6777.
E-mail address: rkpark@wku.ac.kr (R. Park).

http://dx.doi.org/10.1016/j.bbrc.2014.11.070
0006-291X/

cultured in high-glucose DMEM (GIBCO BRL, Grand Island, NY, USA) supplemented with 10% fetal bovine serum (FBS; GIBCO BRL) at 33 °C and 5% CO_2 in humidified atmosphere. Cells were grown in a humidified atmosphere at 37 °C, 5% CO_2. To determine cell viability, cells were treated with MTT (0.5 mg) for 2 h and were washed three times with phosphate buffered saline (PBS, pH 7.4). Insoluble formazan product was dissolved in DMSO and the optical density (OD) of each culture well was measured using a microplate reader (Titertek Multiskan, Flow Laboratories) at 590 nm. The OD of the control cells was taken as 100% viability.

2.2. Organotypic cultures of Corti's organ explants

The organotypic culture procedure was described previously [19]. In short, Sprague Dawley rats were sacrificed on postnatal day two (P3) and the cochlea were carefully dissected. The stria vascularis and the spiral ligament were dissected away leaving the organ of Corti. For further study, the organ of Corti was dissected into three regions of the apical, middle and basal turns. Cochlear explants were treated with DMEM containing glucose (4.5 g/l) and 10% FBS during the stationary phase of cell growth at 12 h post-dissection. Cochlear explants were treated with 5 μM MG132 (Sigma) and bortezomib (Santa Cruz), then incubated for 30 h at 37 °C, 5% CO_2. The control group, maintained with serum containing DMEM medium only, was cultured concurrently with the experimental groups. At the end of the experiment, the cultures were prepared for histological analysis. Organotypic cultures of Corti's organ were fixed in 2% paraformaldehyde in PBS at RT for 20 min. The specimens were rinsed with PBS, then incubated in 0.25% Triton X-100 for 5 min, and immersed in tetramethyl rhodamine isothiocyanate (TRITC)-labeled phalloidin (Sigma, 1:100 diluted) in PBS for 20 min. After rinsing three times with PBS, the specimens were examined under a fluorescence microscope. This work was carried out in conformity with all applicable regulations and institutional use rules of Laboratory Animals in Wonkwang University School of Medicine.

2.3. Western blot analysis

Cells (3×10^6) were scraped off the culture plates and centrifuged at 1000×*g* for 5 min at 4 °C. Cells were homogenized with lysis buffer (10 mM Tris–HCl pH 7.6, 150 mM NaCl, 1% Triton X-100, 1% sodium deoxycholate, 1 mM EDTA, 2.5 mM b-glycerophosphate, 1 mM dithiothreitol, 1 mM NaF, 1 mM Na_3VO_4, 1 mM phenylmethanesulfonylfluoride, and 1× protease inhibitor cocktail) and centrifuged at 14,000 rpm for 10 min at 4 °C, and the supernatant was taken. Cell lysates were heated at 100 °C for 15 min and subject to SDS–PAGE electrophoresis. Separated proteins were electroblotted onto a nitrocellulose membrane. The membrane was then incubated in TBS-T blocking buffer for 1 h and carried out the antibody binding reaction for the first antibody and secondary HRP-conjugated antibody. Antibody against PMP70 was purchased from Thermo Scientific (Rockford, IL, USA). Anti-β-actin antibody was purchased from Santa Cruz Biotech Inc. (Santa Cruz, CA, USA). Anti-catalase antibody was purchased from Rockland (Gilbertsville, PA, USA). After extensive washes, protein bands on the membrane were visualized using an enhanced chemiluminescence detection system (Amersham, Piscataway, NJ, USA) according to the manufacturer's recommended protocol.

2.4. RT-PCR (Q-PCR)

Total RNAs were extracted from cultured cells with TRIzol reagent (Invitrogen). A reverse transcription kit (Roche, Indianapolis, IN) was used to construct the template cDNA for real-time PCR (Q-PCR) with LightCycler using FastStart DNA Master SYBR Green I (Roche, Indianapolis, IN). The primer sequences for mouse cDNAs were as follows:

PMP70-1: 5′-gggagaagcagacaatccac-3′ and reverse, 5′-ccgaaagaa aatgaaattatgtagg-3′, Catalase: forward, 5′-cttcaagttggttaatgcaga-3′ and reverse, 5′-caagtttttgatgccctggt-3′. Pex2: forward, 5′-tga aggaaccacttagaaattacaga-3′ and reverse, 5′-ccagggccttattcagttca-3′. Pex14: forward, 5′-ctcactccgcagccataca-3′ and reverse, 5′-agccaaggcaccataatctc-3′. Pex11α: forward, 5′-ttcatccgagtcgccaac-3′ and reverse, 5′-catgcatgcgtgctgagt-3′. Pex11β: forward, 5′-gagcctc ggacgaaagttg-3′ and reverse, 5′-caggtgcacagccctttt-3′. ACOX1: forward, 5′-agattggtagaaattgctgcaaaa-3′ and reverse, 5′-acgccactt ccttgctcttc-3′. HSD17B4: forward, 5′-gggagcagtacttggagctg-3′ and reverse, 5′-tcagcaataactgcttcacatttt-3′. SCPx: forward, 5′-ggttggct atgatatgagtaaagaagct-3′ and reverse, 5′-agctctatcacgtcgacatcgtt-3′. EHHADH: forward, 5′-ccggtcaatgccatcagt-3′ and reverse, 5′-ctaaccgt atggtccaaactagc-3′. PTHlO: forward, 5′-agagactgcctgactcctatgg-3′ and reverse, 5′-ctgcttctgccgtgaaatg-3′. Internal control 36B4: 5′-cact ggtctaggacccgagaag-3′; and reverse, 5′-ggtgcctctggagattttcg-3′. Each analysis was performed in triplicate.

2.5. Immunofluorescence

Cells were washed with PBS, fixed in 4% paraformaldehyde (Sigma–Aldrich HT5014) at room temperature for 20 min, rinsed in PBS, incubated in 0.1% Triton X-100, and then rinsed in PBS. After incubation in 3% BSA (Bovine Serum Albumin), cells were incubated with 1:400 of target protein antibody at 4 °C. Next, plates were carefully washed with PBS, stained with Alexa flur-568 dye, washed twice with PBS and incubated with 10 μM DAPI in PBS at RT for 30 min. After mounting the coverslip, cells were observed under a fluorescence microscope.

2.6. Preparation of cytosol and membrane fraction tractions

Cells were washed with ice-cold PBS, scraped and centrifuged at 1000×*g* for 5 min at 4 °C. The cell pellet was then homogenated in 400 μl of buffer (10 mM HEPES, pH 7.9, 50 mM NaCl, 0.1 mM EDTA, 0.25 M Sucrose). The homogenates were centrifuged at 1000×*g* for 10 min at 4 °C and the supernatant was transferred a new tube. The supernatant was centrifuged at 13,000×*g* for 30 min at 4 °C. After centrifugation, the supernatant (cytosol fraction) was transferred to a new tube and the pellet (membrane fraction) was resuspended in lysis buffer. Both fractions were used for Western blot analysis.

2.7. Generation of stably transfected HEI-OC1 cells expression RFP-SKL

HEI-CO1 cells were transfected with 2 μg of pRFP-SKL plasmid using X-tremeGENE9 DNA transfection reagent (Roche). 24 h after transfection, cells were switched to a medium supplemented with 700 μg/ml G418 to select for cells expressing a neomycin-containing plasmid. Fresh medium was added every 2–3 days until colonies were formed at ~15 days. Individual colonies were isolated with cloning cylinders, and expression of RFP-SKL was assessed under a fluorescence microscope.

3. Results

To investigate the ototoxic effect of proteasome inhibitor, HEI-OC1 auditory cells were treated for 24 h with various concentrations of MG132, a proteasome inhibitor. As shown in Fig. 1A, MG132 decreased cell viability in a dose-dependent manner. To verify the result from HEI-OC1 cells, we examine the effect of MG132 on sensory hair cells in the primary cultures of organ of Corti isolated from postnatal day 3 (P3) rat. The organ of Corti was treated with 5 μM MG132 for 24 h. After incubation, F-actin

was labeled with TRITC-conjugated phalloidin to visualize stereocilia bundles in the organ of Corti. As shown in Fig. 1B, three rows of the outer hair cells (OHCs) and single row of inner hair cells (IHCs) were clearly visible in control. In contrast, treatment of either MG132 or another proteasome inhibitor, bortezomib, markedly destroyed most stereocilia bundles of hair cells and resulted in the disarrangement of the stereocilia. These data suggest that proteasome inhibitor may induce ototoxicity consistent with recent clinical reports.

To test whether a proteasome inhibitor affects expression of peroxisomal genes, we performed a quantitative real time PCR to measure transcriptional activities of PMP70, PEX2, Pex14, Pex11α, Pex11β, HSD17B4, SCPx, EHHADH, PTHIO and Catalase in HEI-OC1 cells. As shown in Fig. 2A, treatment of MG132 decreased expression of PMP70, PEX2, Pex14, Pex11α, Pex11β, HSD17B4, SCPx, EHHADH, and PTHIO as compared to the control. We also examined the protein levels of Catalase and PMP70 by Western blot analysis. In Fig. 2B, the amount of both Catalase and PMP70 proteins was decreased by the treatment of MG-132 in a time-dependent manner. To examine whether the number of peroxisomes was affected by the treatment of a proteasome inhibitor, we performed immunofluorescence with antibody against PMP70 in HEI-OC1 cells. As shown in Fig. 2C, treatment of either MG-132 or bortezomib reduced the number of peroxisomes as compared to untreated control cells. These data suggest that proteasome may play an important role in peroxisome functions in HEI-OC1 cells by regulating expression of peroxisomal proteins as well as peroxisome biogenesis.

One of the important roles of the peroxisome is lipid metabolism such as fatty acid oxidation. Accordingly, previous reports showed that peroxisome dysfunction induced by Pex5 knockout or a depletion of Acox1, a peroxisome beta-oxidation gene, led to accumulation of lipid droplets [20,21]. Since the treatment of proteasome inhibitors in HEI-OC1 cells impairs both the number and expression of peroxisome genes, we examined whether proteasome inhibitors affect fatty acid oxidation by measuring the intracellular triglyceride (TG) accumulation. We treated proteasome inhibitors, either MG132 or bortezomib, and measured lipid droplet (LD) formation by BODIPY staining in HEI-OC1 cells. As shown in Fig. 3A, we detected highly accumulated LD in cells treated with either MG-132 or bortezomib, as compared to that in untreated control cells. Oleic acids treatment was used as a positive control. We also performed a similar experiment ex vivo using the organ of Corti explants. As shown in Fig. 3B, LD was accumulated in the explants by the treatment of proteasome inhibitors. These data suggest that the treatment of proteasome inhibitors may induce TG accumulation possibly by interfering with peroxisome functions.

The import of PTS1-containing peroxisomal matrix proteins is mediated by the PTS1 receptor protein, Pex5, which is subjected to ubiquitination by Pex2 and Pex12. Although the exact mechanism needs to be elucidated, monoubiquitinated Pex5 is destined for a new round of the receptor recycle, while polyubiquitinated Pex5 is degraded by the proteasome. To examine whether a proteasome inhibitor blocks the Pex5-dependent import system of PTS1-containing peroxisomal matrix proteins, we examined subcellular distribution of Catalase, a well-known peroxisomal matrix protein. HEI-CO1 cells were treated with MG132 for 6–12 h, and then fractionated into the membrane and cytosol fractions. As shown in Fig. 4A, treatment of MG132 decreased the amount of Catalase in the membrane fraction but increased in the cytosol fraction, implicating Catalase to be largely detected in the cytosol To rule out the possibility that the effect of MG132 is specific only to Catalase, we generated a HEI-CO1 cell line which stably expresses RFP-SKL (Red Fluorescent Protein efficiently imported into the peroxisome in a Pex5-dependent manner) and tested whether MG132 also affects peroxisomal localization of RFP-SKL. As shown in Fig. 4B, RFP-SKL displayed a peroxisomal localization in the absence of MG132. However, RFP-SKL was mainly detected in the cytosol upon the treatment of MG132. These data indicate that a proteasome inhibitor, MG132, blocks the import pathway of PTS1-peroxisome matrix proteins in HEI-OC1 cells.

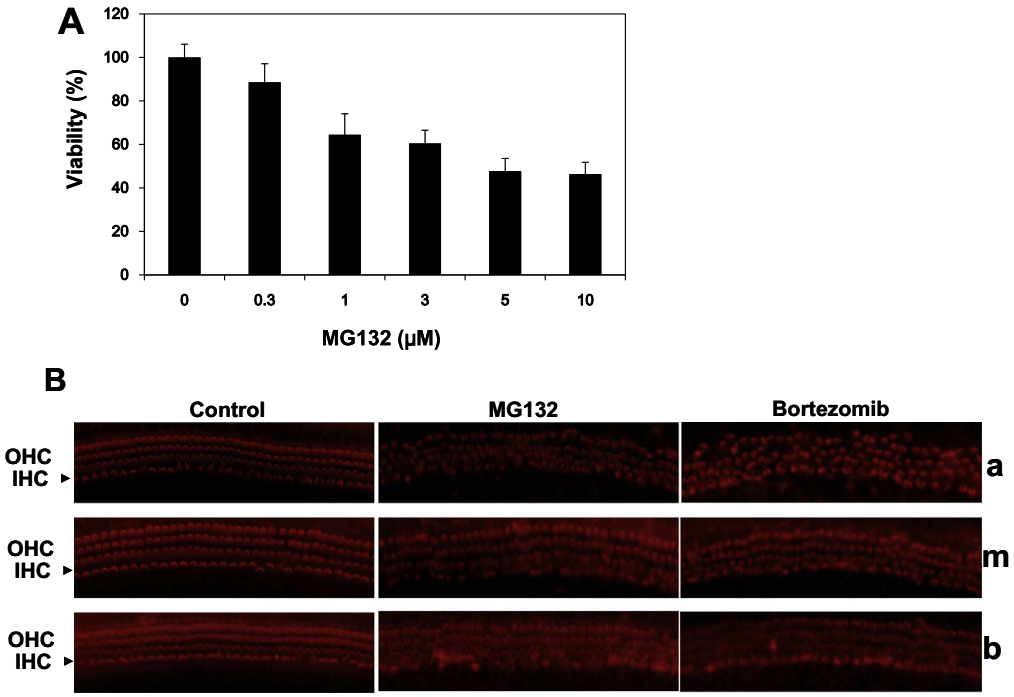

Fig. 1. Proteasome inhibition affects viability of hair cells in vitro and ex vivo. (A) HEI-OC1 cells treated with indicated concentration of MG132 for 24 h were assayed for viability by MTT. (B) The organ of Corti explants from post-natal day 3 rats were treated with DMSO, 5 μM MG132, or 5 μM Bortezomib for 24 h. The explants were stained with TRITC-conjugated phalloidin and then observed under a fluorescence microscope. OHC; outer hair cell, IHC; inner hair cell, a; apical turn, m; middle turn, b; basal turn.

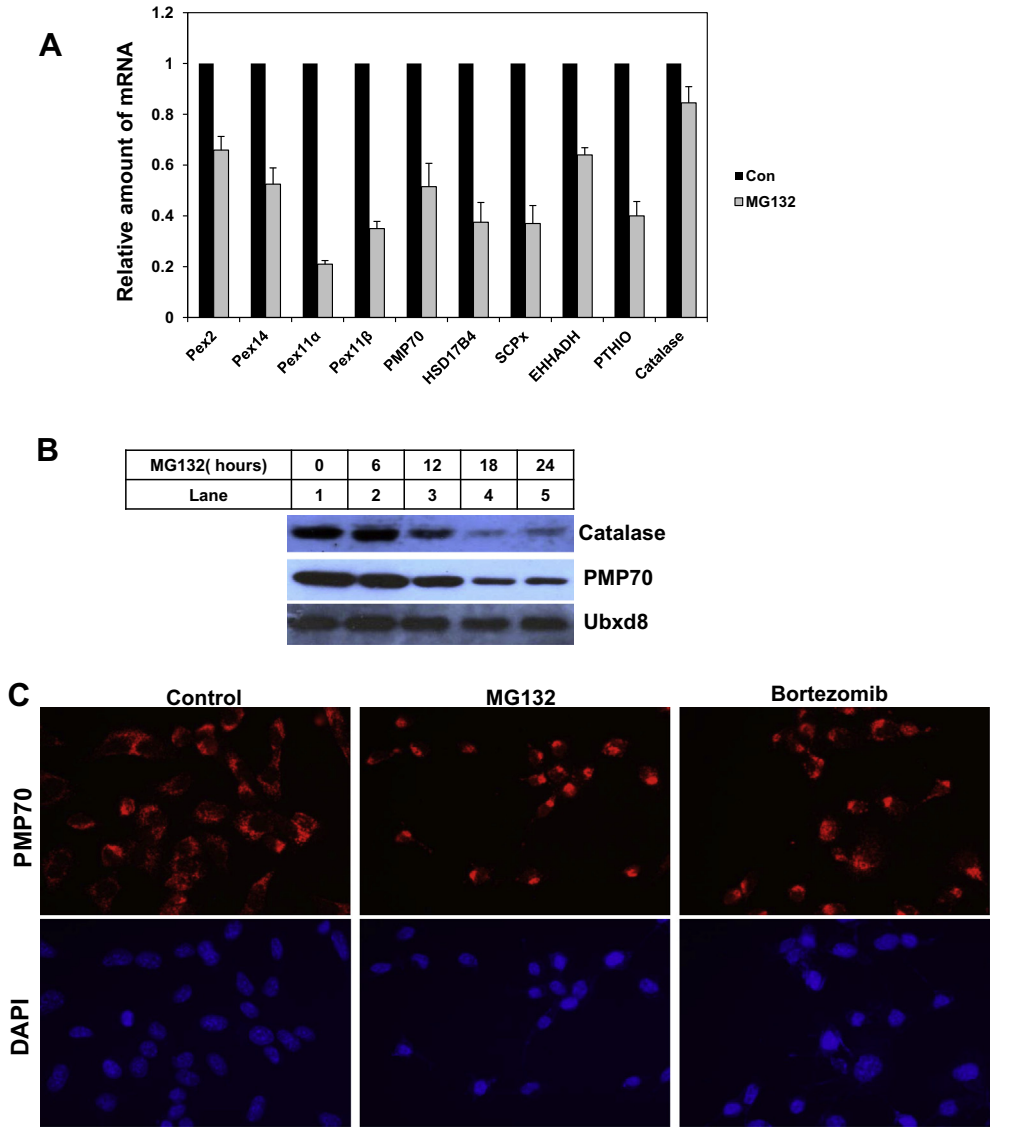

Fig. 2. Treatment of a proteasome inhibitor induces peroxisome dysfunction in HEI-OC1 cells. (A) HEI-OC1 cells were treated with 5 μM MG132 for 16 h. Total RNA was isolated and real time quantitative PCR was conducted. (B) Cells were treated with 5 μM MG132 for the indicated time. Cells were then harvested and membrane fraction from cell lysate was subjected to SDS–PAGE followed by immunoblot analysis using antibodies against Catalase, PMP70, and Ubxd8. (C) HEI-OC1 cells were treated with 5 μM MG132 or 5 μM bortezomib for 16 h. After incubation, cells were fixed and immunostained with anti-PMP70 for detecting peroxisomes and DAPI for nucleus. Cells were observed under a fluorescence microscope.

4. Discussion

In this study, we demonstrated that proteasome inhibitors induce damage in the auditory HEI-OC1 cells and the organ of Corti explants. We also showed that proteasome inhibition affects the function of the peroxisome by decreasing both peroxisomal protein expression and the number of peroxisomes. Furthermore, our data revealed that import of peroxisome matrix proteins is also blocked by the treatment of proteasome inhibitors. The dysfunction of the peroxisome might be associated with cellular lipid droplet accumulation by preventing peroxisomal fatty acid degradation in the auditory HEI-OC1 cells and the organ of Corti explants.

Intracellular protein degradation regulated by the ubiquitin-proteasome pathway is critical to various cellular processes, and this inhibition of proteasome function is known to be associated with cellular damage, which in turn may induce cell death [11]. For peroxisome biogenesis, the ubiquitin-proteasome pathway is also crucial for importing the peroxisomal matrix proteins. The peroxisomal import apparatus can mediate the transport of peroxisome matrix proteins through the peroxisomal membrane, although the detailed mechanisms still need to be defined. Based on the model of the cycling receptor, peroxisomal matrix proteins are recognized in the cytosol by a receptor protein which interacts with the docking complexes located in the surface of the peroxisomal membrane. After interaction between receptor and docking complexes, the matrix proteins are delivered into the peroxisomal matrix, and finally, the receptor is released from the peroxisomal membrane in an ATP-dependent manner and then subject to either proteasomal degradation or recycling for next round of the import. Pex5, a PTS1 protein receptor, delivers various matrix proteins into peroxisome, and is known to be mono- or polyubiquitinated [22–24]. Three Peroxins, Pex2, Pex10 and Pex12, contain a C-terminal RING (really interesting new gene) finger domain which has been implicated to act as an E3 ubiquitin ligase. Our result showed that the treatment of proteasome inhibitors block peroxisomal import of Catalase and RFP-PTS1, implying that the Pex5-dependent

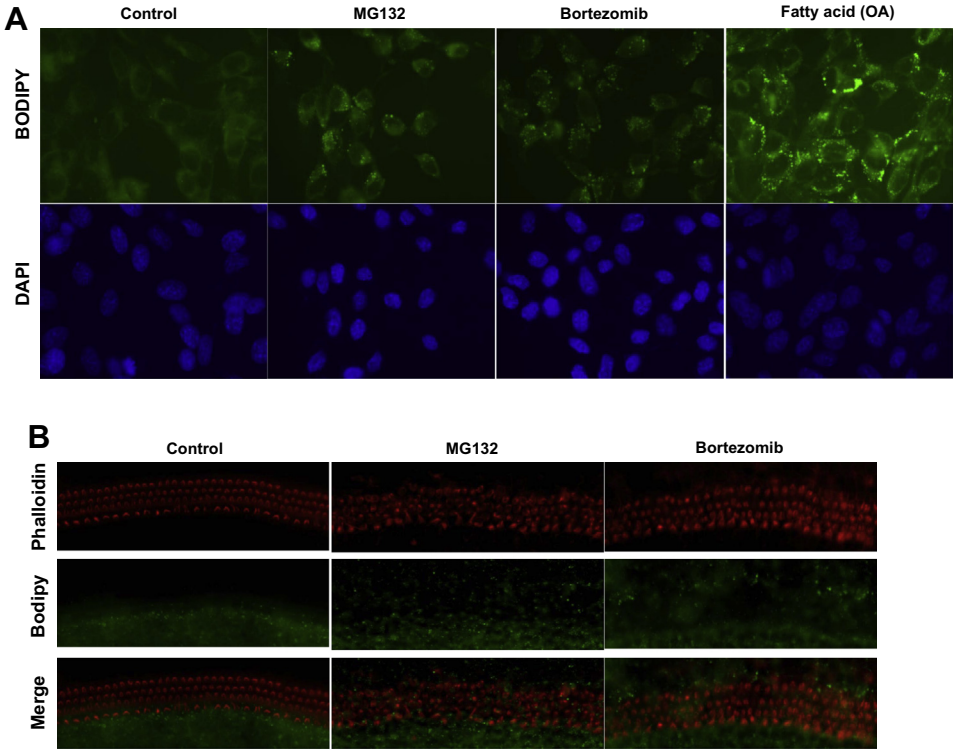

Fig. 3. Proteasome inhibition increases accumulation of lipid droplets in vitro and ex vivo. (A) HEI-OC1 cells were treated with either 100 μM oleic acid, 5 μM MG132, or 5 μM bortezomib for 16 h. Lipid droplets in the cells were visualized by BODIPY staining. (B) The organ of Corti explants from post-natal day 3 rats were treated with DMSO, 5 μM MG132, or 5 μM Bortezomib for 24 h. The explants were stained with TRITC-conjugated phalloidin and BODIPY and observed under a fluorescence microscope.

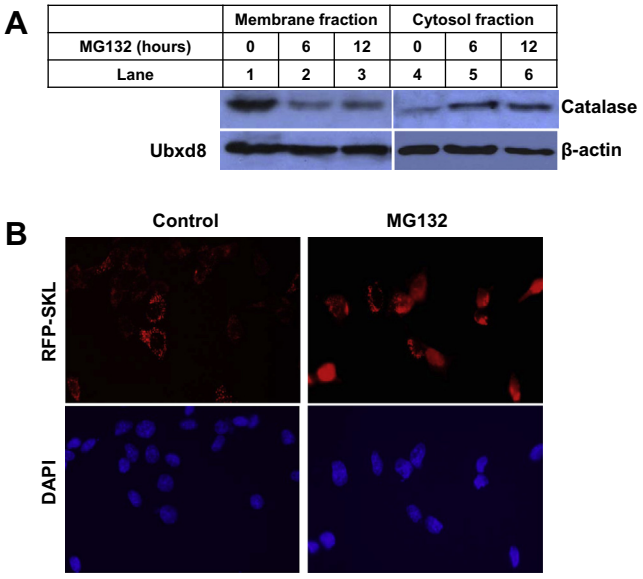

Fig. 4. Impaired proteasome blocks the import of peroxisomal matrix proteins in HEI-OC1 cells. (A) HEI-OC1 cells treated with 5 μM MG132 for the indicated time were harvested and separated into the membrane and cytosol fractions. Lysates were subjected to SDS–PAGE followed by immunoblot analysis. (B) HEI-OC1 cells expressing RFP-SKL were treated with 5 μM MG132 for 16 h. After incubation, cells were fixed and RFP signal was observed under a fluorescence microscope.

peroxisomal import pathway is largely blocked by proteasome inhibition.

The use of ototoxic drugs, such as cisplatin or aminoglycoside antibiotics, leads to ROS accumulation in the inner ear [25,26] and the continuous accumulation of ROS leads primarily to the damage of inner ear cells and the death of innervating neurons [27]. Also, acoustic trauma has been proven to be a major cause of ROS production in the cochlea which may lead eventually to hearing loss [28]. Interestingly, various proteasome inhibitors including MG132 have been reported to stimulate apoptotic cell death through ROS accumulation [29]. Recent clinical reports suggest that the therapy with a proteasome inhibitor is also associated with bilateral hearing loss [13,14]. Although the precise mechanism by which proteasome inhibitors induce ototoxicity needs to be defined, it is possible that peroxisome damage caused by proteasome inhibition might be related to ototoxicity through ROS accumulation. Notably, a sensorineural deafness is a common feature of all classic peroxisome biogenesis disorder (PBD) phenotypes as well as some of peroxisome enzyme disorder (PED) phenotypes. In addition, it is implicated that peroxisome dysfunction may cause ROS accumulation associated with hearing loss. Our finding of the damage of auditory HEI-OC1 cells and the organ of Corti explants upon the treatment of proteasome inhibitors strongly suggests that proteasome inhibition may impair normal peroxisomal function which in turn induces auditory cell damage.

Disclosure

All the authors declared no competing interests.

Acknowledgment

This work was supported by Wonkwang University in 2012.

References

[1] R.J.A. Wanders, H.R. Waterham, Biochemistry of mammalian peroxisomes revisited, Annu. Rev. Biochem. 75 (2006) 295–332.
[2] M. Islinger, S. Grille, H.D. Fahimi, M. Schrader, The peroxisome: an update on mysteries, Histochem. Cell Biol. 137 (2012) 547–574.

[3] M. Fidaleo, Peroxisomes and peroxisomal disorders: the main facts, Exp. Toxicol. Pathol. 62 (2010) 615–625.
[4] S.J. Steinberg, G. Dodt, G.V. Raymond, N.E. Braverman, A.B. Moser, H.W. Moser, Peroxisome biogenesis disorders, Biochim. Biophys. Acta 1763 (2006) 1733–1748.
[5] P.P. Van Veldhoven, Biochemistry and genetics of inherited disorders of peroxisomal fatty acid metabolism, J. Lipid Res. 51 (2010) 2863–2895.
[6] C. Ma, G. Agrawal, S. Subramani, Peroxisome assembly: matrix and membrane protein biogenesis, J. Cell Biol. 193 (2011) 7–16.
[7] X. Liu, C. Ma, S. Subramani, Recent advances in peroxisomal matrix protein import, Curr. Opin. Cell Biol. 24 (2012) 484–489.
[8] A. Hershko, A. Ciechanover, The ubiquitin system for protein degradation, Annu. Rev. Biochem. 61 (1992) 761–807.
[9] D. Voges, P. Zwickl, W. Baumeister, The 26S proteasome: a molecular machine designed for controlled proteolysis, Annu. Rev. Biochem. 68 (1999) 1015–1068.
[10] A.L. Goldberg, T.N. Akopian, A.F. Kisselev, D.H. Lee, M. Rohrwild, New insights into the mechanisms and importance of the proteasome in intracellular protein degradation, Biol. Chem. 378 (1997) 131–140.
[11] R.Z. Orlowski, The role of the ubiquitin-proteasome pathway in apoptosis, Cell Death Differ. 6 (1999) 303–313.
[12] P. Perez-Galan, G. Roue, N. Villamor, E. Montserrat, E. Campo, D. Colomer, The proteasome inhibitor bortezomib induces apoptosis in mantle-cell lymphoma through generation of ROS and Noxa activation independent of p53 status, Blood 107 (2006) 257–264.
[13] C.S. Chim, L.G. Wong, Deafness associated with the use of Bortezomib in multiple myeloma, Acta Oncol. 47 (2008) 323–324.
[14] M. Engelhardt, A.M. Müller, W. Maier, R. Wäsch, Severe irreversible bilateral hearing loss after bortezomib (VELCADE) therapy in a multiple myeloma (MM) patient, Leukemia 19 (2005) 869–870.
[15] E.M. Bleeker-Wagemakers, J.W.E. Oorthuys, R.J.A. Wanders, R.B.H. Schutgens, Long term survival of a patient with the cerebro-hepato-renal (Zellweger) syndrome, Clin. Genet. 29 (1986) 160–164.
[16] R.J.A. Wanders, Metabolic and molecular basis of peroxisomal disorders, Am. J. Hum. Genet. 126 (2004) 355–375.
[17] S. Ferdinandusse, S. Denis, E.M. Hogenhout, J. Koster, C.W.T. van Roermund, L. IJlst, A.B. Moser, R.J.A. Wanders, H.R. Waterham, Clinical, biochemical, and mutational spectrum of peroxisomal acyl-coenzyme A oxidase deficiency, Hum. Mutat. 28 (2007) 904–912.
[18] S.B. Pierce, T. Walsh, K.M. Chisholm, M.K. Lee, A.M. Thornton, A. Fiumara, J.M. Opitz, E. Levy-Lahad, R.E. Klevit, M.C. King, Mutations in the DBP-deficiency protein HSD17B4 cause ovarian dysgenesis, hearing loss, and ataxia of Perrault syndrome, Am. J. Hum. Genet. 87 (2010) 282–288.
[19] J.L. Zheng, W.Q. Gao, Differential damage to auditory neurons and hair cells by ototoxins and neuroprotection by specific neurotrophins in rat cochlear organotypic cultures, Eur. J. Neurosci. 8 (1996) 1897–1905.
[20] R. Dirkx, I. Vanhorebeek, K. Martens, A. Schad, M. Grabenbauer, D. Fahimi, P. Declercq, P.P. Van Veldhoven, M. Baes, Absence of peroxisomes in mouse hepatocytes causes mitochondrial and ER abnormalities, Hepatology 41 (2005) 868–878.
[21] C.Y. Fan, J. Pan, R. Chu, D. Lee, K.D. Kluckman, N. Usuda, I. Singh, A.V. Yeldandi, M.S. Rao, N. Maeda, J.K. Reddy, Hepatocellular and hepatic peroxisomal alterations in mice with a disrupted peroxisomal fatty acyl-coenzyme A oxidase gene, J. Biol. Chem. 271 (1996) 24698–24710.
[22] M.O. Debelyy, H.W. Platta, D. Saffian, A. Hensel, S. Thoms, H.E. Meyer, B. Warscheid, W. Girzalsky, R. Erdmann, Ubp15p, a ubiquitin hydrolase associated with the peroxisomal export machinery, J. Biol. Chem. 286 (2011) 28223–28234.
[23] T. Francisco, T.A. Rodrigues, M.O. Freitas, C.P. Grou, A.F. Carvalho, C. Sá-Miranda, M.P. Pinto, J.E. Azevedo, A cargo-centered perspective on the PEX5 receptor-mediated peroxisomal protein import pathway, J. Biol. Chem. 288 (2010) 29151–29159.
[24] H.W. Platta, F. El Magraoui, B.E. Baumer, D. Schlee, W. Girzalsky, R. Erdmann, Pex2 and Pex12 function as protein-ubiquitin ligases in peroxisomal protein import, Mol. Cell. Biol. 29 (2009) 5505–5516.
[25] W.J. Clerici, K. Hensley, D.L. DiMartino, D.A. Butterfield, Direct detection of ototoxicant-induced reactive oxygen species generation in cochlear explants, Hear. Res. 98 (1996) 116–124.
[26] B. Sergi, A. Ferraresi, D. Troiani, G. Paludetti, A.R. Fetoni, Cisplatin ototoxicity in the guinea pig: vestibular and cochlear damage, Hear. Res. 182 (2003) 56–64.
[27] B. Bánfi, B. Malgrange, J. Knisz, K. Steger, M. Dubois-Dauphin, K.M. Krause, NOX3, a superoxide-generating NADPH oxidase of the inner ear, J. Biol. Chem. 279 (2004) 46065–46072.
[28] K.K. Ohlemiller, J.S. Wright, L.L. Dugan, Early elevation of cochlear reactive oxygen species following noise exposure, Audiol. Neurootol. 4 (1999) 229–236.
[29] Y.H. Ling, L. Liebes, Y. Zou, R. Perez-Soler, Reactive oxygen species generation and mitochondrial dysfunction in the apoptotic response to Bortezomib, a novel proteasome inhibitor, in human H460 non-small cell lung cancer cells, J. Biol. Chem. 278 (2003) 33714–33723.